Mechanism and Machine Theory 45 (2010) 1520–1536

Contents lists available at ScienceDirect

Mechanism and Machine Theory

journal homepage: www.elsevier.com/locate/mechmt

Study on involute of circle with variable radii in a scroll compressor

Yangguang Liu [a], Chinghua Hung [a,*], Yuchoung Chang [b]

[a] Department of Mechanical Engineering, National Chiao Tung University, Taiwan
[b] Energy & Environment Research Laboratories, Industrial Technology Research Institute, Taiwan

ARTICLE INFO

Article history:
Received 22 February 2010
Received in revised form 25 June 2010
Accepted 2 July 2010
Available online 3 August 2010

Keywords:
Scroll compressor
Involute of circle
Variable radii

ABSTRACT

A geometric model of scroll profiles, constructed from an involute of circle with variable radii, has been developed by using the theorem of planar orbiting mechanisms. Parametric studies have also been investigated in this study. When compared to the conventional scroll profile with the same suction volume, volume ratio and housing size, this new model demonstrates better reliability and efficiency because of a lower wrap height. Alternatively, a scroll type compressor with a more compact housing size can be achieved by using this new profile but keeping its wrap height the same as the conventional one. Furthermore, arc and line modifications have been built to provide wider design varieties. These are used to avoid interference at the center of the scroll pair and to boost the volume ratio of this new scroll profile.

1. Introduction

The scroll type compressor (STC) is an efficient, quiet, simple, and reliable rotary machine that has been under development since the 1970s. It's a kind of positive displacement compressor. The basic principle of the STC, which is a combination of a compression process with an orbiting motion, is made up of two key components—fixed scroll and orbiting scroll. At first, the orbiting scroll is rotated 180° (π rad) relative to the stationary fixed scroll, and is then coupled with a crank mechanism to orbit the fixed scroll at a constant radius. In addition, an anti-rotation coupling is joined to the orbiting scroll to prevent it from rotating as it orbits. From this motion, several volumes in the enclosed chambers in between the two scroll parts can be gradually decreased and moved inward from the periphery to the center portion. As such, the working media in these chambers can be compressed smoothly and finally be discharged from a discharge port at the center of the fixed scroll to complete one compression and discharge process.

With regard to the scroll pair (which are the fixed and orbiting scrolls), numerous technical papers and patents have been written and proposed, to improve STC performance. From a geometric viewpoint, many curve profiles that have been used to create the scroll pair (such as the involute of circle, archimedes spirals and segmental arcs) have been investigated continuously in literature [1–4]. In addition, Lee et al. [5] proved that several theorems related to planar orbiting mechanisms can be used to design a scroll pair. Some methods and modifications have also been presented for reaching the perfectly meshing engagement at the center of the scroll pair, thus avoiding the mutual interference and improving its efficiency [6–8]. Also, Li et al. [9] compared the advantages and defects of different curves that can be used to form the scroll wrap profiles in STC. In the mathematic field of the theoretic study, a planar curve expressed by the intrinsic equation has also been developed to derive a closed analytical expression regarding several scroll profiles [10–12].

Furthermore, several studies using eco-friendly refrigerant (ex. CO_2) in STC have garnered much attention in recent years. But this means that the STC must confront with higher pressure conditions resulted from the specific operating temperatures. Due to this, developing a scroll pair with better rigidity and strength to endure these high pressure conditions has become an issue. Among the literature about the involute scroll profiles, a new type constructed from an involute of circle with variable radii was

* Corresponding author. National Chiao Tung University, EE452, 1001 Ta Hsueh Road, Hsinchu, Taiwan, 300. Tel.: +886 3 5712121 55160; fax: 886 3 5720634.
E-mail addresses: ygliu.me94g@nctu.edu.tw (Y. Liu), chhung@mail.nctu.edu.tw (C. Hung).

0094-114X/$ – see front matter © 2010 Elsevier Ltd. All rights reserved.
doi:10.1016/j.mechmachtheory.2010.07.001

Nomenclature

a	radius of base circle (mm)
a_0	initial radius of base circle (mm)
C_0, C_1	contact points
C_{in}, C_{ou}	joint points
D_m	minimum endplate diameter of the orbiting scroll (mm)
d,d'	distance used in arc and line modification (mm)
h	wrap height of the scroll pair (mm)
k	polytropic index
r_{ob}	orbiting radius (mm)
R, R'	radius of the modified arcs (mm)
V	volume (mm^3)
V_{SUC}	suction volume (mm^3)
V_{DIS}	discharge volume (mm^3)
Vol_r	volume ratio
x, y	coordinate
$\prod_f$, $\prod_m$	coordinate planes
ψ	independent angle parameter (rad)
α	starting involute angle (rad)
β	modified angle between the outer and inner involute curve (°, rad)
δ_0	corrected increment (mm)
γ	derivative angle (rad)
σ	derivative angle (rad)
ρ	radius of curvature (mm)
Δr	modified distance (mm)
ϕ	involute angle of scroll (rad)
ϕ_E,ϕ_D	ended involute angle (rad); corresponding involute angle at discharge (rad)
θ,θ_D	orbiting angle of scroll (rad); orbiting angle at discharge (rad)

Subscripts

c	center position
in	inner curve
ou	outer curve

proposed for higher efficiency, reliability and wider design freedom [13,14]. However, the illustration of this new type of scroll profile lacks specifics. Its advantages and defects have not yet been explained clearly. Therefore, in this study, a complete geometric model of the scroll profiles constructed from an involute of circle with variable radii will be formulated and proved by utilizing the theorem of planar orbiting mechanisms [5]. After that, several case studies will be implemented and important values regarding this geometric model will be discussed. Furthermore, two types of perfectly meshing modifications—arc and line shapes to the center portion of this new scroll profile—as well as their formulations, uses and restrictions, will also be presented.

2. Geometric model of the scroll profile constructed from an involute of circle with variable radii

The complete mathematic expressions will be delineated in the following paragraphs. However, the theorem of planar orbiting mechanisms [5] must first be reviewed and understood clearly.

2.1. Theorem of planar orbiting mechanisms

Theorem 1 [5]: Whenever two curves, one in plane $\prod_f$ and the other in plane $\prod_m$, make contact, the contact point must be on the concave side of the curve. This is called the inner curve and the convex side of the other curve is called the outer curve. The difference between the radius of curvature (ρ) of the two curves must be equal to the orbiting radius (r_{ob}) at all points of contact.

This theorem can be explained, as shown in Fig. 1, by considering the origins of the two planes, $\prod_f$ and $\prod_m$, as they orbit around each other, and one smooth curve in plane $\prod_m$, which can be expressed as

$$\begin{cases} x_m = x_c(\psi_m) + \rho(\psi_m)cos\psi_m \\ y_m = y_c(\psi_m) + \rho(\psi_m)sin\psi_m. \end{cases} \quad (1)$$

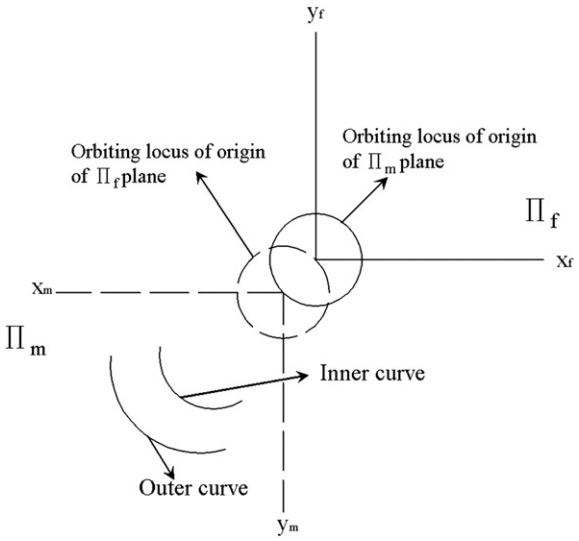

Fig. 1. Illustration: theorem of planar orbiting mechanisms.

Then a pair of outer and inner conjugate curves can be expressed in plane $\prod_f$ as follows

$$\begin{cases} x_{f,ou} = -x_c(\psi_m) - [\rho(\psi_m) + r_{ob}]cos\psi_m \\ y_{f,ou} = -y_c(\psi_m) - [\rho(\psi_m) + r_{ob}]sin\psi_m \end{cases} \tag{2}$$

$$\begin{cases} x_{f,in} = -x_c(\psi_m) - [\rho(\psi_m) - r_{ob}]cos\psi_m \\ y_{f,in} = -y_c(\psi_m) - [\rho(\psi_m) - r_{ob}]sin\psi_m \end{cases} \tag{3}$$

when $\rho(\phi_m) - r_{ob} \geq 0$.

It's also been found that the outer and inner curves expressed by Eqs. (2) and (3) in plane $\prod_f$ respond to the inner and outer conjugate curves that were expressed by the Eq. (1) in plane $\prod_m$. Due to the two planes being rotated 180° ($\psi_f = \psi_m \pm \pi$) toward each other, Eqs. (2) and (3) can also be expressed in plane $\prod_f$ as follows

$$\begin{cases} x_{f,ou} = -x_c(\psi_f - \pi) - [\rho(\psi_f - \pi) + r_{ob}]cos(\psi_f - \pi) \\ y_{f,ou} = -y_c(\psi_f - \pi) - [\rho(\psi_f - \pi) + r_{ob}]sin(\psi_f - \pi) \end{cases} \tag{4}$$

$$\begin{cases} x_{f,in} = -x_c(\psi_f + \pi) - [\rho(\psi_f + \pi) - r_{ob}]cos(\psi_f + \pi) \\ y_{f,in} = -y_c(\psi_f + \pi) - [\rho(\psi_f + \pi) - r_{ob}]sin(\psi_f + \pi). \end{cases} \tag{5}$$

This theorem distinctly shows that the coordinates of the conjugate curves are related to center position (x_c, y_c), the radius of the curvature (ρ), the orbiting radius (r_{ob}) and the independent variable (ψ).

2.2. Conceptual illustration and formulations

2.2.1. Conceptual illustration

The basic illustration is shown in Fig. 2. The conventional scroll curve is constructed from an involute of circle with a fixed radius (a). This adds to the radius of the curvature (ρ) at each point of the curve. However, the biggest difference between the conventional scroll curve and the one addressed in this study is that the two parameters (a and ρ) have both been changed by the

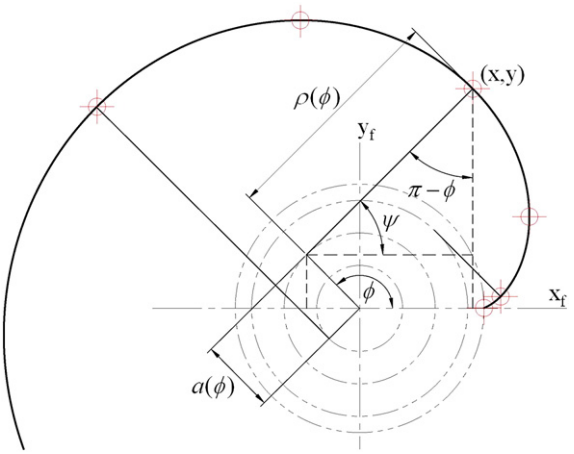

Fig. 2. Sketch map and parametric definitions of an involute of circle with variable radii.

involute angle (ϕ). By replacing independent variable ψ with the coordinate relation $\psi=\phi-\pi/2$ (as shown in Fig. 2), and applying the method of vector projection and trigonometric geometry, the planar coordinates to this involute can be expressed in Cartesian coordinates as:

$$\begin{cases} x = \rho(\phi)\cdot cos(\psi) - a(\phi)\cdot sin(\psi) = \rho(\phi)\cdot cos\left(\phi-\frac{\pi}{2}\right) - a(\phi)\cdot sin\left(\phi-\frac{\pi}{2}\right) \\ \quad = a(\phi)\cdot cos(\phi) + \rho(\phi)\cdot sin(\phi) \\ y = \rho(\phi)\cdot sin(\psi) + a(\phi)\cdot cos(\psi) = \rho(\phi)\cdot sin\left(\phi-\frac{\pi}{2}\right) + a(\phi)\cdot cos\left(\phi-\frac{\pi}{2}\right) \\ \quad = a(\phi)\cdot sin(\phi) - \rho(\phi)\cdot cos(\phi). \end{cases} \tag{6}$$

If a is a constant value, Eq. (6) represents the conventional involute which is used in most of scroll machinery. If both a and ρ are varied with the involute angle ϕ ($a=a(\phi)$, $\rho=\rho(\phi)$), various forms can be further exploited. One of these, the polytropic expression as it relates to the involute angle ϕ, can be devised and expressed as follows:

$$\begin{aligned} a &= a(\phi) = a_0 + \delta_0\phi^k \\ \rho &= \rho(\phi) = \int_0^{\phi} (a_0 + \delta_0\phi^k)d\phi = a_0\phi + \frac{\delta_0}{k+1}\phi^{k+1} \end{aligned} \tag{7}$$

k is the polytropic index. a_0 and δ_0 represent the initial radius of the base circle and the corrected increment. One conventional involute can be obtained when $\delta_0=0$. If $\delta_0>0$ or $\delta_0<0$, the distance between the two curves, which correspond to the thickness of the scroll pair, will be increased or decreased toward the peripheral of the scroll wrap.

2.2.2. Formulation

By utilizing Eqs. (6) and (7) and transforming the parametric relations as shown in Fig. 3, the outer involute with the involute angle ϕ at the contact point C_0 in plane $\prod_f$ can be expressed as

$$\begin{cases} x_{f,ou} = a_{ou}\cos\phi + \rho_{ou}\sin\phi \\ y_{f,ou} = a_{ou}\sin\phi - \rho_{ou}\cos\phi \end{cases} \tag{8}$$

where

$$\begin{aligned} a_{ou} &= a_{ou}(\phi) = a_0 + \delta_0\phi^k \\ \rho_{ou} &= \rho_{ou}(\phi) = a_0\phi + \frac{\delta_0}{k+1}\phi^{k+1}. \end{aligned} \tag{9}$$

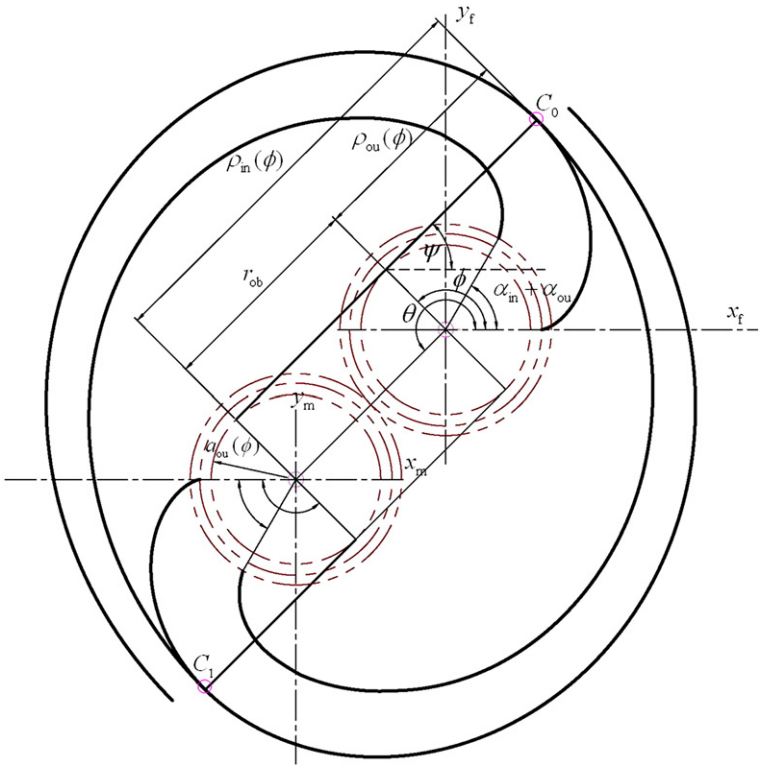

Fig. 3. Parametric relations of the scroll profiles constructed from an involute of circle with variable radii.

By assuming the starting involute angles α_{in}, α_{ou} for the inner and outer curves respectively, and referring to Fig. 3, the contact relation can be derived once the inner curve in plane $\prod_f$ expands $\phi' = \phi + \pi - (\alpha_{in} + \alpha_{ou})$ angles. Due to the necessary condition that "a pair of conjugate curves have a common radius of a base circle" must be satisfied, a and ρ for the inner curves at contact point C_1 must be expressed as follows:

$$\begin{aligned} a_{in} &= a_{ou}(\phi) = a_{in}(\phi') \\ &= a_0 + \delta_0[\phi' - (\pi - \alpha_{in} - \alpha_{ou})]^k|_{\phi' = \phi + \pi - (\alpha_{in} + \alpha_{ou})} \\ &= a_0 + \delta_0\phi^k \\ \rho_{in} = \rho_{in}(\phi') &= \int_0^{\phi'} \{a_0 + \delta_0[\phi' - (\pi - \alpha_{in} - \alpha_{ou})]^k\} d\phi' \\ &= (a_0\phi')|_0^{\phi + \pi - (\alpha_{in} + \alpha_{ou})} + \{\frac{\delta_0}{k+1}[\phi' - (\pi - \alpha_{in} - \alpha_{ou})]^{k+1}\}|_0^{\phi + \pi - (\alpha_{in} + \alpha_{ou})} \\ &= a_0[\phi + (\pi - \alpha_{in} - \alpha_{ou})] + \frac{\delta_0}{k+1}[\phi^{k+1} + (-1)^{k+2}(\pi - \alpha_{in} - \alpha_{ou})^{k+1}]. \end{aligned} \tag{10}$$

Then the inner curve in plane $\prod_f$ can be expressed as:

$$\begin{cases} x_{f,in} = a_{in}\cos(\phi + \pi) + \rho_{in}\sin(\phi + \pi) \\ y_{f,in} = a_{in}\sin(\phi + \pi) - \rho_{in}\cos(\phi + \pi) \end{cases} \tag{11}$$

From Theorem 1 in Section 2.1 and Fig. 3, the conjugate outer curve in plane $\prod_m$ can be derived easily from Eqs. (3) to (6) and stated as follows:

$$\begin{cases} x_{f,ou} = x_{m,in} = -x_{f,in} + r_{ob}cos\theta \\ y_{f,ou} = y_{m,in} = -y_{f,in} + r_{ob}sin\theta. \end{cases} \tag{12}$$

The orbiting angle θ, which defines the orbiting relation for planes $\prod_f$ and $\prod_m$ and depends on independent variable ψ or involute angle ϕ, can be derived by letting the *Jacobian* of Eq. (12) equal zero, which is shown as follows:

$$\begin{aligned} Jacobian &= \frac{\partial(x_{m,in}, y_{m,in})}{\partial(\phi, \theta)} = \begin{vmatrix} \frac{\partial x_{m,in}}{\partial \phi} & \frac{\partial y_{m,in}}{\partial \phi} \\ \frac{\partial x_{m,in}}{\partial \theta} & \frac{\partial y_{m,in}}{\partial \theta} \end{vmatrix} \\ &= -(\kappa\delta_0\phi^{k-1} + \rho_{in})(cos\phi \cdot cos\theta + sin\phi \cdot sin\theta) = 0. \end{aligned} \tag{13}$$

Therefore

$$-\frac{cos\phi}{sin\phi} = \frac{sin(\phi + (m + 1/2)\pi)}{cos(\phi + (m + 1/2)\pi)} = \frac{sin\theta}{cos\theta};\ \text{where}\ m = 0, 1, 2.... \tag{14}$$

The orbiting angle θ can then be derived from Eq. (14) or by referring to Fig. 3. It is expressed below:

$$\theta = \psi + \pi = \phi + \pi/2. \tag{15}$$

The corresponding outer curve can be expressed as:

$$\begin{cases} x_{f,ou} = x_{m,in} = -x_{f,in} + r_{ob}cos(\phi + \pi/2) \\ y_{f,ou} = y_{m,in} = -y_{f,in} + r_{ob}sin(\phi + \pi/2). \end{cases} \tag{16}$$

Eqs. (8) and (16), which represent the conjugate curves, can be rearranged to compare the coefficients, and then the orbiting radius r_{ob} can be expressed as follows:

$$r_{ob} = a_0(\pi - \alpha_{in} - \alpha_{ou}) + \frac{\delta_0}{k+1}(-1)^{k+2}(\pi - \alpha_{in} - \alpha_{ou})^{k+1}. \tag{17}$$

2.3. Application for different k values

From the previous description, various curves for different k values can be investigated. By setting the same starting angles to the outer and inner curves, i.e. $\alpha_{ou} = \alpha_{in} = \alpha$, four feasible types of involutes have been constructed in the following statement.

1. $k = 0$

Let $k = 0$ and use Eqs. (9) and (10), Eqs. (8) and (11) (the outer and inner curves in plane $\prod_f$) can be then expressed as:

$$\begin{cases} x_{f,ou} = (a_0 + \delta_0)\cdot\cos\phi + (a_0 + \delta_0)\cdot\phi\cdot\sin\phi \\ y_{f,ou} = (a_0 + \delta_0)\cdot\sin\phi - (a_0 + \delta_0)\cdot\phi\cdot\cos\phi \end{cases} \tag{18}$$

$$\begin{cases} x_{f,in} = (a_0 + \delta_0)\cdot\cos(\phi + \pi) + (a_0 + \delta_0)\cdot(\phi + \pi - 2\alpha)\cdot\sin(\phi + \pi) \\ y_{f,in} = (a_0 + \delta_0)\cdot\sin(\phi + \pi) - (a_0 + \delta_0)\cdot(\phi + \pi - 2\alpha)\cdot\cos(\phi + \pi) \end{cases}. \tag{19}$$

It is easy to find that Eqs. (18) and (19) are the involutes of circle with a fixed radius ($a = a_0 + \delta_0$), and the orbiting radius is

$$r_{ob} = a_0(\pi - 2\alpha) + \delta_0(\pi - 2\alpha) = (a_0 + \delta_0)(\pi - 2\alpha). \tag{20}$$

2. $k = 1$

Let $k = 1$ and follow the same procedure, and the outer and inner curves become

$$\begin{cases} x_{f,ou} = (a_0 + \delta_0\phi)\cdot\cos\phi + (a_0\phi + \frac{\delta_0}{2}\phi^2)\cdot\sin\phi \\ y_{f,ou} = (a_0 + \delta_0\phi)\cdot\sin\phi - (a_0\phi + \frac{\delta_0}{2}\phi^2)\cdot\cos\phi \end{cases} \tag{21}$$

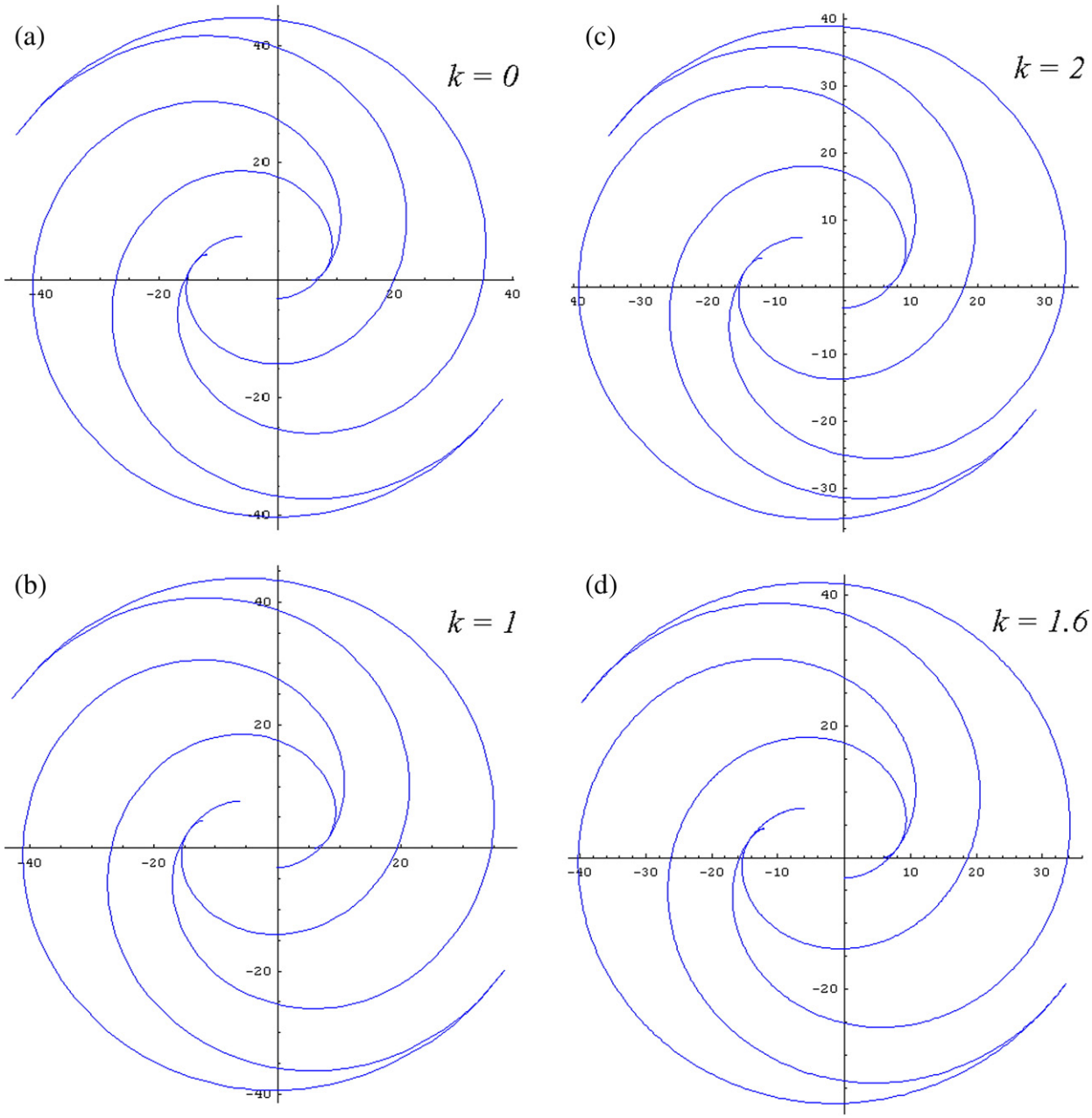

Fig. 4. Sketch map of the scroll profiles for different k values.

$$\begin{cases} x_{f,in} = (a_0 + \delta_0\phi)\cdot\cos(\phi + \pi) \\ \qquad + [a_0(\phi + \pi - 2\alpha) + \dfrac{\delta_0}{2}(\phi^2 - (\pi - 2\alpha)^2)]\cdot\sin(\phi + \pi) \\ y_{f,in} = (a_0 + \delta_0\phi)\cdot\sin(\phi + \pi) \\ \qquad - [a_0(\phi + \pi - 2\alpha) + \dfrac{\delta_0}{2}(\phi^2 - (\pi - 2\alpha)^2)]\cdot\cos(\phi + \pi). \end{cases} \tag{22}$$

Then the orbiting radius can be expressed as

$$r_{ob} = a_0(\pi - 2\alpha) - \frac{\delta_0}{2}(\pi - 2\alpha)^2. \tag{23}$$

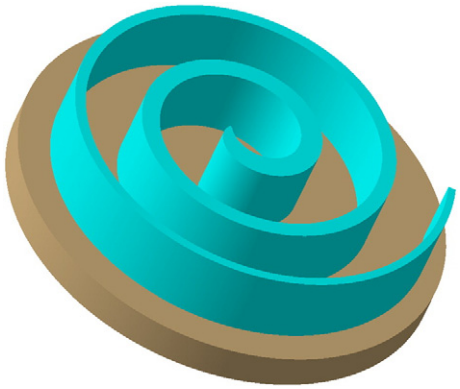

Fig. 5. Structure of orbiting scroll ($k=1$, $\alpha=50°$ and $\delta_0=-0.05$ mm).

3. $k=2$

Let $k=2$ and follow the same procedure, and the outer and inner curves are

$$\begin{cases} x_{f,ou} = (a_0+\delta_0\phi^2)\cdot\cos\phi + (a_0\phi+\frac{\delta_0}{3}\phi^3)\cdot\sin\phi \\ y_{f,ou} = (a_0+\delta_0\phi^2)\cdot\sin\phi-(a_0\phi+\frac{\delta_0}{3}\phi^3)\cdot\cos\phi \end{cases} \tag{24}$$

$$\begin{cases} x_{f,in} = (a_0+\delta_0\phi^2)\cdot\cos(\phi+\pi) \\ \qquad + [a_0(\phi+\pi-2\alpha)+\frac{\delta_0}{3}(\phi^3+(\pi-2\alpha)^3)]\cdot\sin(\phi+\pi) \\ y_{f,in} = (a_0+\delta_0\phi^2)\cdot\sin(\phi+\pi) \\ \qquad -[a_0(\phi+\pi-2\alpha)+\frac{\delta_0}{3}(\phi^3+(\pi-2\alpha)^3)]\cdot\cos(\phi+\pi) \end{cases} \tag{25}$$

and the orbiting radius is

$$r_{ob} = a_0(\pi-2\alpha)+\frac{\delta_0}{3}(\pi-2\alpha)^3. \tag{26}$$

4. $k\neq$ integer

If $k\neq$ integer, the planar coordinates of the conjugate curves and the orbiting radius include complex numbers (because of the term $(-1)^{k+2}$ in Eq. (10)). However, if the real value was adopted only, the conjugate pair can still be created. Let $k=1.6$, then the outer and inner curves, and the orbiting radius will be as follows:

$$\begin{cases} x_{f,ou} = (a_0+\delta_0\phi^{1.6})\cdot\cos\phi + (a_0\phi+\frac{\delta_0}{2.6}\phi^{2.6})\cdot\sin\phi \\ y_{f,ou} = (a_0+\delta_0\phi^{1.6})\cdot\sin\phi-(a_0\phi+\frac{\delta_0}{2.6}\phi^{2.6})\cdot\cos\phi \end{cases} \tag{27}$$

$$\begin{cases} x_{f,in} = (a_0+\delta_0\phi^2)\cdot\cos(\phi+\pi) \\ \qquad + a_0(\phi+\pi-2\alpha)+\frac{\delta_0}{2.6}(\phi^{2.6}+\mathrm{Re}[(-1)^{3.6}](\pi-2\alpha)^{2.6})\cdot\sin(\phi+\pi) \\ y_{f,in} = (a_0+\delta_0\phi^2)\cdot\sin(\phi+\pi) \\ \qquad -a_0(\phi+\pi-2\alpha)+\frac{\delta_0}{2.6}(\phi^{2.6}+\mathrm{Re}[(-1)^{3.6}](\pi-2\alpha)^{2.6})\cdot\cos(\phi+\pi) \end{cases} \tag{28}$$

$$r_{ob} = a_0(\pi-2\alpha)+\frac{\delta_0}{2.6}\mathrm{Re}[(-1)^{3.6}](\pi-2\alpha)^{2.6}. \tag{29}$$

The involutes for the four cases discussed above are shown in Fig. 4. Fig. 5 exhibits the structure of the orbiting scroll where $k=1$, $\alpha=50°(5\pi/18)$ and $\delta_0=-0.05$(mm).

Table 1
Combinations of design parameters and related results.

	Unit	A0	A1	A2	A3	A4
Design parameters						
ϕ_E	rad	16.755	16.755	16.755	16.755	16.755
α	rad	0.785	0.733	0.785	0.820	0.855
a_0	mm	1.9099	2	2.1	2.2	2.3
a_0/δ_0	–	–	−167	−89	−62	−49
h	mm	5.19	4.56	4.525	4.428	4.357
Results						
V_{suc}	mm^3	4500	4500	4500	4500	4500
V_{dis}	mm^3	1960	1960	1960	1960	1960
Vol_r	–	2.3	2.3	2.3	2.3	2.3
r_{ob}	mm	3	3.3	3.3	3.3	3.3
D_m	mm	73.00	73.02	73.09	73.05	73.02
Wrap volume	mm^3	4160	3123	3140	3027	2951

2.4. Volume calculations

The analytic expression to volume calculation of the case $k=1$ with the same starting angles ($\alpha_{ou}=\alpha_{in}=\alpha$) has been derived. By considering the coordinate expressions of Eqs. (11) and (13), the enclosed chamber areas formed from the scroll pair can be calculated as follows:

$$\begin{aligned} A &= \frac{1}{2}\int_{\phi-2\pi}^{\phi}\left|x_{m,in}\cdot\frac{d(y_{m,in})}{d\phi}-y_{m,in}\cdot\frac{d(y_{m,in})}{d\phi}\right|d\phi \\ &\quad -\frac{1}{2}\int_{\phi-2\pi}^{\phi}\left|x_{f,ou}\cdot\frac{d(y_{f,ou})}{d\phi}-y_{f,ou}\cdot\frac{d(y_{f,ou})}{d\phi}\right|d\phi \\ &= -\frac{1}{12}\pi(\pi-2\alpha)[-2a_0+(\pi-2\alpha)\delta_0]\cdot \\ &\quad \{-6a_0(\pi+2\alpha-2\phi)+\delta_0[5\pi^2+12\pi(\alpha-\phi)+6(\phi^2-2\alpha^2)]\} \end{aligned} \tag{30}$$

ϕ represents the involute angle that responds to the contact point of the inner curve. By assuming the symmetrical chambers in a scroll pair, the chamber volume, the variation of it with ϕ and the suction volume V_{SUC} can be expressed as follows:

$$\begin{aligned} V(\phi) = {} & -(h/6)\pi(\pi-2\alpha)[-2a_0+(\pi-2\alpha)\delta_0]\cdot \\ & \{-6a_0(\pi+2\alpha-2\phi)+\delta_0[5\pi^2+12\pi(\alpha-\phi)+6(\phi^2-2\alpha^2)]\} \end{aligned} \tag{31}$$

$$\begin{aligned} \frac{dV(\phi)}{d\phi} = {} & -(h/6)\pi(\pi-2\alpha)[-2a_0+(\pi-2\alpha)\delta_0]\cdot \\ & [12a_0+\delta_0(-12\pi+12\phi)] \end{aligned} \tag{32}$$

$$V_{SUC} = V(\phi_E) \tag{33}$$

ϕ_E is the ended involute angle of the scroll pair. It follows that the volume ratio is

$$Vol_r = V(\phi_E)/V(\phi_D) \tag{34}$$

ϕ_D represents the corresponding involute angle at where the discharge step has been designed to arrive. The analytic expression to the volume calculation for the other k values or a different starting angle $\alpha_{ou}\neq\alpha_{in}$ can also be constructed in accordance with the above-mentioned procedure.

3. Parametric study and discussion

Several cases of scroll profiles constructed from the involutes of circle with both constant and variable radii are compared. These cases are regarding the condition that the polytropic index $k=1$, and for simplicity, the same starting angles $\alpha_{ou}=\alpha_{in}=\alpha$ are used for the inner and outer involutes.

3.1. Comparison based on fixed suction volume, volume ratio and housing size

The scroll pair with symmetrical chambers has been used with respect to the two different scroll profiles. Important design specifications in STC, such as the suction volume V_{SUC} and volume ratio Vol_r are fixed as 4500 mm^3 and 2.3 in this case. These

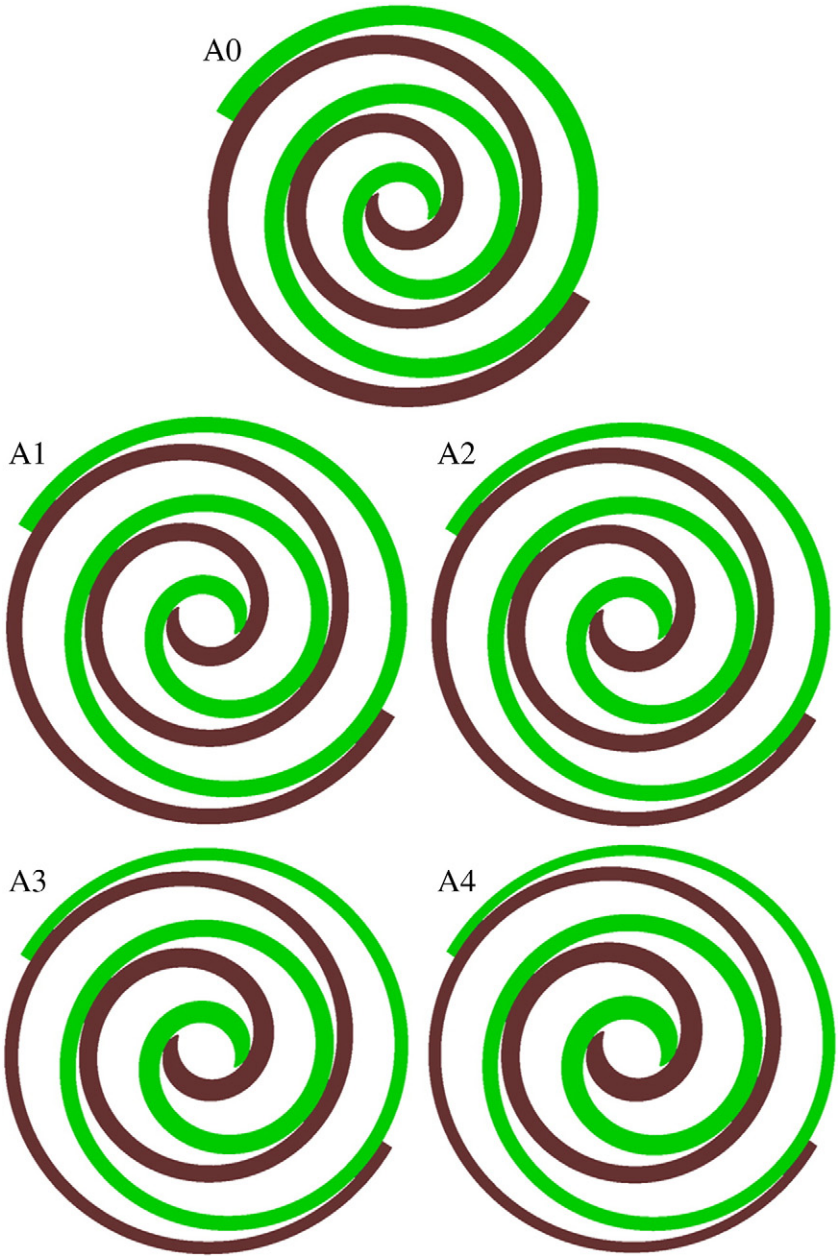

Fig. 6. Scroll profiles from A0 to A4.

fixed values must be maintained to satisfy the design specifications. Also, the endplate of the orbiting scroll with a suitable diameter D_m must be designed to match up with the limitation of the housing size for STC. This minimum D_m can be calculated approximately as

$$D_m = 2[\rho_{ou}(\phi_E + \alpha) + r_{ob}] = 2[a_0 \cdot (\phi_E + \alpha) + 1/2 \cdot \delta_0 \cdot (\phi_E + \alpha)^2 + r_{ob}]. \quad (35)$$

Therefore, the new type of scroll pair must hold the same D_m as the conventional one.

According to the model of this new type, four design combinations with different a_0, δ_0 and α values (shown in Table 1) have been calculated. The V_{SUC}, Vol_r and D_m were kept the same as the conventional type.

The key design parameters and important results for the conventional scroll profile (A0) and these four combinations (A1 to A4) are all shown in Table 1. Fig. 6 displays the derived scroll profiles from A0 to A4. Fig. 7(a) shows that these four combinations can also lower the wrap height at a ratio from 12.1% to 16.1%. In addition, the wrap volume can also be reduced by −24.9% to

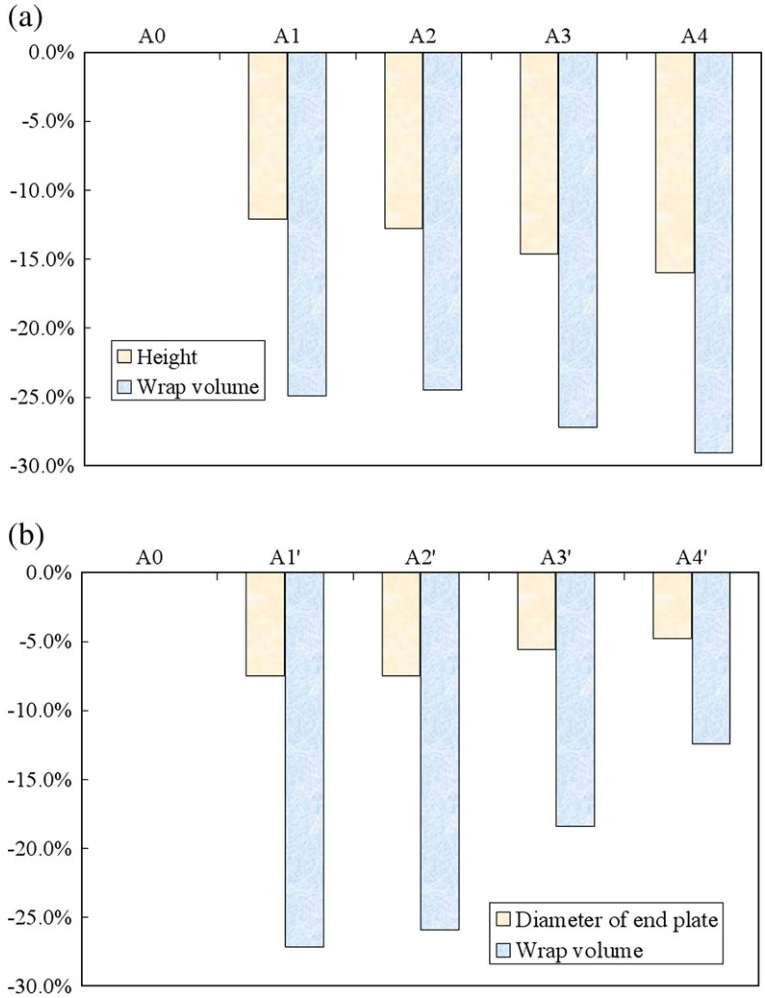

Fig. 7. Reduction ratio in A1 to A4 and A1′ to A4′, A0 as standard. (a) Scroll wrap height and wrap volume (A1 to A4). (b) Diameter of the end-plate and wrap volume (A1′ to A4′).

−29.1%. Even though the orbiting radius r_{ob} of the four combinations is bigger than that of the conventional one, the minimum endplate radius D_m can still be approximately the same. Therefore, the limitation of housing size will not be an issue.

Though having the same V_{SUC} and Vol_r, a smaller wrap height h in STC is a significant improvement. When the orbiting scroll rotates to compress the refrigerant, the gas forces that are created by the pressure differences between adjacent chambers and exerted on the scroll wrap, will be proportional to the wrap height and give rise to the bending moment on the scroll wrap. Obviously, a bigger bending moment not only generates higher stress on the root part but also causes bigger deformation on the top part of the scroll wrap. Since the higher stress will result in the possibility of fracture and durability issues, and a bigger deformation will lead to severe leakage between adjacent chambers, it will eventually degrade the compressor's efficiency. By changing the wrap height to as low as possible, and using the same design specifications for STC, these two drawbacks can both be reduced.

Increasing attention has been paid to harmless and eco-friendly refrigerants all over the world in recent years due to the threats of ozone depletion and global warming problems. Therefore, some working fluids (as shown in Table 2) like HFC compounds (ex. R407C and R410A) with zero ODP values and some natural refrigerants with lower GWP values (ex. CO_2) have gradually been used to replace the conventional CFC and HCFC refrigerants. However, the needed pressure conditions that correspond to the specified

Table 2
ODP/GWP values to several refrigerants.

Name	R12	R22	R407C	R410A	CO2
Compositions	CFC	HCFC	HFC	HFC	Natural gas
ODP (ozone depletion potential)	1	0.055	0	0	0
GWP (global warming potential)	8100	1810	1700	1975	1

operating temperatures used in the refrigeration and air-conditioning field for these substitutes, such as R410A and CO_2, are 1.5 and 5 times higher compared to the conventional refrigerants (ex. R22). Hence the scroll pair must confront higher pressure differences with these substitutes. In the light of this, the design of the scroll pair to suit these refrigerants must be reconsidered further.

If the conventional design of the scroll profile remains unchanged, higher stress and deformation levels on the scroll wraps could be generated and the durability and efficiency of the scroll pair in STC could be degraded more by adopting these eco-friendly refrigerants. By applying these new types of the scroll profile (for example, $k=1$ and $\alpha_{ou}=\alpha_{in}=\alpha$), once the thickness in the inward portion of the scroll wrap, which bears the higher fluid pressure, can be increased and that in the outward portion, which bears the lower pressure, can be decreased, the rigidity and strength of the new type of the scroll wrap can be improved. Then the advantages induced by this new scroll profile can be observed more distinctly.

3.2. Comparison based on fixed suction volume, volume ratio and wrap height

If the material used in the scroll pair is suitably selected with greater strength and rigidity, then the wrap height h can still hold to the same value as the conventional one. Even so, in order to satisfy the fixed V_{SUC} and Vol_r values, other design parameters such as ϕ_E, a_0, δ_0 and α, need to be adjusted once more. Similarly, four other design combinations (A1′ to A4′) are also listed in Table 3. Fig. 7(b) shows that these four combinations can reduce D_m from 4.8% to 7.5%. The wrap volume can be reduced by −12.5% to −27.2%. The orbiting radius r_{ob} to the four combinations is also a little different when compared to the conventional one.

The smaller D_m with the same V_{SUC} and Vol_r becomes an important factor, even though the rate of the decreasing D_m in this case is smaller than the rate of the decreasing wrap height h in the previous case. The smaller D_m implies that the smaller housing size, which is compared to conventional STC, can accomplish the same V_{SUC} and Vol_r. Therefore, a more compact size of STC with the same capacity and volume ratio can provide wider freedom in design consideration by using the involute of circle with variable radii.

4. Perfectly meshing modification at the center of the scroll profile

Similar to the conventional scroll profiles, the perfectly meshing modifications for avoiding interference at the center portion of the scroll profile, still needs to be addressed. Based on the references [6,7] and [15–17], it is found that the arc and line modifications are both easy to understand and convenient to be translated into CAM (computer-aided-manufacturing) procedures. These two modifications will be formulated in detail later.

4.1. Arc modification of involutes of circle with variable radii

Two respective arc curves can be used to join the inner and outer involutes when modifying them. In order to guarantee the meshing engagement (with the same tangential slope or holding first-order continuous at the joint of two curves), the following three necessary conditions must be satisfied [16,17]:

1. The joining of one arc curve with the outer involute must be first-order continuous.
2. The joining of the other arc curve with the inner involute must be first-order continuous.
3. The joining of these two arc curves must be first-order continuous.

4.1.1. Formulation

For the involute of circle with variable radii, the contact relation between the two arc curves and the involutes must be illustrated in order to formulate their mathematic relations. As shown in Fig. 8, let β be a modified angle that corresponds to the center curve between the outer and inner involutes and C_{ou} represent the joint point of the arc and the outer involute. Similarly, let

Table 3
Combinations of design parameters and related results.

	Unit	A0	A1′	A2′	A3′	A4′
Design parameters						
ϕ_E	rad	16.755	16.319	16.319	16.232	16.232
α	rad	0.785	0.794	0.845	0.895	0.935
a_0	mm	1.9099	2	2.1	2.2	2.3
a_0/δ_0	–	–	−82	−58	−51	−44
h	mm	5.19	5.19	5.19	5.19	5.19
Results						
V_{suc}	mm^3	4500	4500	4500	4500	4500
V_{dis}	mm^3	1960	1960	1960	1960	1960
Vol_r	–	2.3	2.3	2.3	2.3	2.3
r_{ob}	mm	3	3.1	3.1	3	2.9
D_m	mm	73	67.5	67.5	68.9	69.5
Wrap volume	mm^3	4160	3029	3081	3392	3642

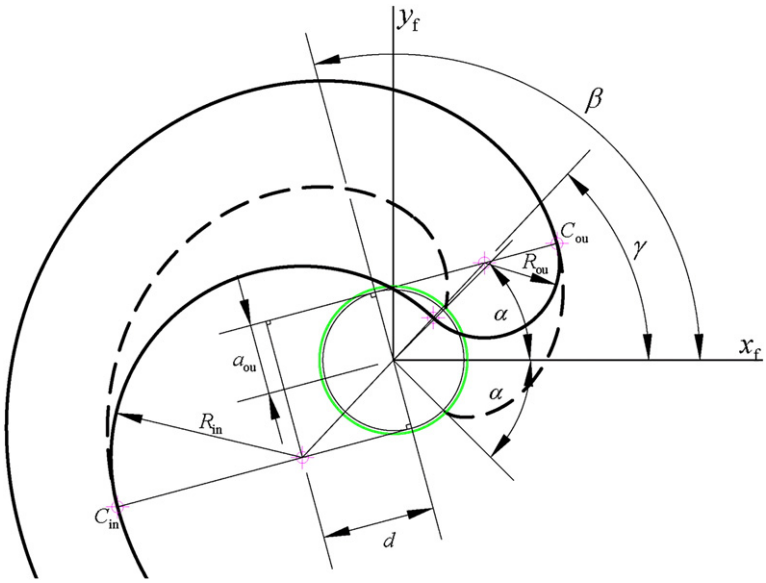

Fig. 8. Parametric definitions of the arc modification.

angle $\beta+\pi$ be another corresponding angle and let C_{in} represent the joint point of the arc and the inner involute. By leading those two arc curves to the center portion and applying the theorem of planar orbiting mechanisms [5] and trigonometry [16], the relations can be expressed as follows:

$$(R_{in} + R_{ou})^2 - (2a_{ou})^2 = (2d)^2 \tag{36}$$

$$d = \rho_{ou} - R_{ou} \tag{37}$$

$$R_{in} - R_{ou} = r_{ob}. \tag{38}$$

R_{ou} and R_{in} represent the radius of the two arc curves that connect to the outer and inner involute curves. a_{ou} and ρ_{ou} represent the radius of the base circle and the radius of curvature at contact point C_{ou}. The formulation can be expressed as:

$$\begin{aligned} a_{ou} &= [a_0 + \delta_0(\beta + \alpha)^k] \\ \rho_{ou} &= [a_0(\beta + \alpha) + (-1)^{k+2}\frac{\delta_0}{k+1}(\beta + \alpha)^{k+1}]. \end{aligned} \tag{39}$$

Using Eq. (39) and solving Eqs. (36) to (38), important relations can be obtained as follows:

$$R_{ou} = [a_0(\beta + \alpha) + (-1)^{k+2}\frac{\delta_0}{k+1}(\beta + \alpha)^{k+1}] - d \tag{40}$$

$$R_{in} = R_{ou} + r_{ob} \tag{41}$$

$$d = \frac{[a_0(\beta + \alpha) + (-1)^{k+2}\frac{\delta_0}{k+1}(\beta + \alpha)^{k+1} + \frac{r_{ob}}{2}]^2 - [a_0 + \delta_0(\beta + \alpha)^k]^2}{2[a_0(\beta + \alpha) + (-1)^{k+2}\frac{\delta_0}{k+1}(\beta + \alpha)^{k+1} + \frac{r_{ob}}{2}]}. \tag{42}$$

The corresponding parameters, the derivative angle γ and the orbiting angle at the discharge moment θ_D (as shown in Fig. 8) can then be expressed as

$$\gamma = \beta - tan^{-1}\left(\frac{d}{a_{ou}}\right). \tag{43}$$

$$\theta_D = 2\pi - \gamma$$

Finally, the parametric expressions of the two arc curves (R_{ou} and R_{in}) are

$$\begin{cases} x_{R_{ou}} = R_{ou}\cdot cos\theta + \sqrt{a_{ou}^2 + d^2}\cdot cos\gamma \\ R_{ou} = R_{ou}\cdot sin\theta + \sqrt{a_{ou}^2 + d^2}\cdot sin\gamma \end{cases};\ \theta\in\left[\gamma-\pi,\beta-\frac{\pi}{2}\right] \tag{44}$$

$$\begin{cases} x_{R_{in}} = R_{in}\cdot cos\theta + \sqrt{a_{ou}^2+d^2}\cdot cos(\gamma+\pi) \\ R_{in} = R_{in}\cdot sin\theta + \sqrt{a_{ou}^2+d^2}\cdot sin(\gamma+\pi) \end{cases};\ \theta\in\left[\gamma,\beta+\frac{\pi}{2}\right]. \tag{45}$$

4.1.2. Discussion

Several related constraint conditions from these parameters must be considered once the arc modification has been applied. These include:

1. $R_{ou}>0$: the outer arc curve exists if $R_{ou}>0$, otherwise the tip point could happen (if $R_{ou}\leq 0$) at the joint of the outer involute and the inner arc curve, so the stress concentration could arise in the tip of the scroll wraps.
2. $\beta>-\alpha$ guarantees the existence of an intersection between the outer arc and the outer involute curve.
3. Larger β value means larger R_{ou} and R_{in} values, which represents a thicker wrap profile at the center portion.

Several arc curves with corresponding R_{ou} and R_{in} can be derived to assist this modification by choosing a different modified angle β. Fig. 9 shows the modifications when β is set as 65°(13π/36), 85°(17π/36), 105°(21π/36), 125°(25π/36), 145°(29π/36) and 165°(33π/36). From Eq. (43) and Fig. 9, it is found that when a lower β angle is used, a bigger orbiting angle at the discharge moment (θ_D) can be obtained while still keeping the same values of the other parameters, which means the planar orbiting motion can reach the discharge step much later. Hence the volume ratio (V_{SUC}/V_{DIS}) can be raised substantially and if possible, surpass the needed design requirements for the designated operating conditions (pressure ratio or compression ratio) of STC. Owing to this, some defects (e.g. over-compression) may occur during the compression step and consume unnecessary work. Furthermore, the volume ratio for different β angle with both modifications of involutes of circle with variable radii is similar to that with a fixed radius [15–17].

4.2. Line modification of involutes of circle with variable radii

This modification uses two conjugate straight lines to collocate with two arc curves to achieve a perfect mesh. By doing this, the increased level of the volume ratio (V_{SUC}/V_{DIS}) can be lowered when compared with the arc modification.

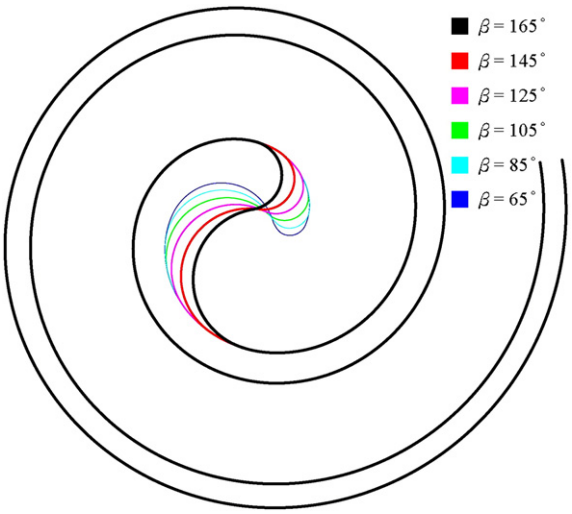

Fig. 9. Comparison of different β values to the scroll profile with arc modification.

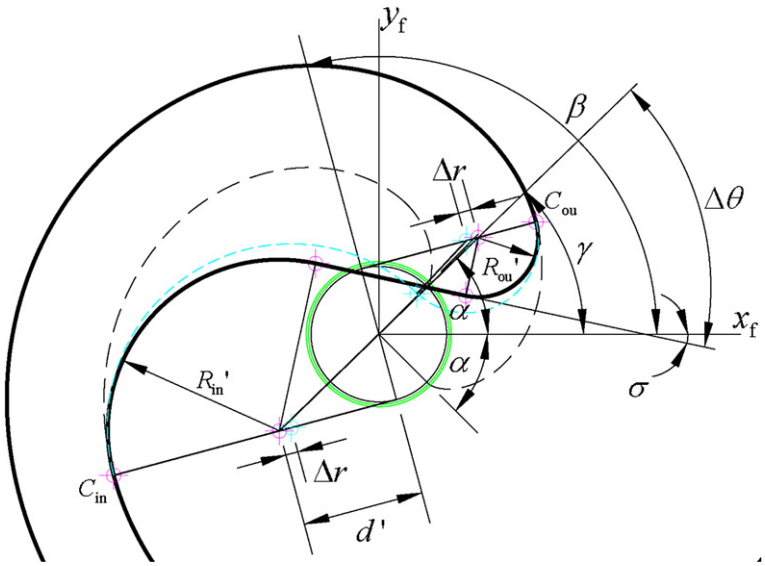

Fig. 10. Parametric definitions of the line modification.

4.2.1. Formulation

In addition to the modified angle β, another parameter Δr (as shown in Fig. 10), called the modified distance, must be introduced into this modification. From Eq. (38), it is known that the difference between the radii of the inner and outer arcs must be equal to the orbiting radius ($R_{in}-R_{ou}=r_{ob}$). This equation can also be rewritten as follows [16]

$$(R_{in}-\Delta r)-(R_{ou}-\Delta r)=R_{in}^{'}-R_{ou}^{'}=r_{ob}. \tag{46}$$

The planar orbiting motion and perfect conjugate mesh are still maintained because of the unchanged r_{ob} value. As shown in Fig. 10, the modified parameters are expressed below

$$\begin{aligned} R_{in}^{'} &= R_{in}-\Delta r \\ R_{ou}^{'} &= R_{ou}-\Delta r \\ d^{'} &= d+\Delta r. \end{aligned} \tag{47}$$

Therefore, the derivative angle γ is

$$\gamma=\beta-tan^{-1}\left(\frac{d^{'}}{a_{ou}}\right). \tag{48}$$

Another derivative angle $\Delta\theta$, defined by the included angle between the modified line and the connecting line between the center of the two arc curves, can be expressed as

$$\Delta\theta=sin^{-1}\left(\frac{R_{in}^{'}+R_{ou}^{'}}{2\sqrt{a_{ou}^{2}+d^{'2}}}\right). \tag{49}$$

In addition, another derivative angle σ, defined by the included angle between the modified line and the coordinate x_f axis (shown in Fig. 10) is

$$\sigma=\gamma-\Delta\theta. \tag{50}$$

Then the orbiting angle at the moment of discharge can be expressed as

$$\theta_D=2\pi-\left(\sigma+\frac{\pi}{2}\right). \tag{51}$$

Finally, the parametric expressions of the two arc curves (R'_{ou} and R'_{in}) are

$$\begin{cases} x_{R'_{ou}} = R'_{ou}\cdot cos\theta + \sqrt{a_{ou}^2 + d'^2}\cdot cos\gamma \\ y_{R'_{ou}} = R'_{ou}\cdot sin\theta + \sqrt{a_{ou}^2 + d'^2}\cdot sin\gamma \end{cases} ;\ \theta\in\left[\sigma-\pi,\beta-\frac{\pi}{2}\right] \tag{52}$$

$$\begin{cases} x_{R'_{in}} = R'_{in}\cdot cos\theta + \sqrt{a_{ou}^2+d'^2}\cdot cos(\gamma+\pi) \\ R'_{in} = R'_{in}\cdot sin\theta + \sqrt{a_{ou}^2+d'^2}\cdot sin(\gamma+\pi) \end{cases} ;\ \theta\in\left[\sigma,\beta+\frac{\pi}{2}\right]. \tag{53}$$

4.2.2. Discussion

The parameter Δr will affect the modified scroll profile in addition to the modified angle β. When changing Δr values, three results are shown below.

1. $\Delta r = 0$: the same effect as the arc curves modification is achieved.
2. $0 \le \Delta r \le R_{ou}$: one straight line joins the two arc curves as the modified profile. When $\Delta r = R_{ou}$, only one straight line can connect the inner arc curve, the outer curve does not exist.
3. $\Delta r > R_{ou}$: line modification cannot be accomplished because of interference.

By keeping the other parameter values the same and setting $\beta = 105°(21\pi/36)$ and varying Δr from 0 to 1.5 mm (as an example), the changes of the modified scroll profile are shown in Fig. 11(a).

It is found that once $\Delta r > 0$, then θ_D is smaller than that by using arc modification. Moreover, the bigger Δr used, the earlier the discharge step will be reached (because of smaller θ_D). Therefore the corresponding volume ratio can be designed according to specified requirements. On the other hand, the result of constant Δr(0.5 mm) and variable β values (65°~165°(13π/36~33π/36))

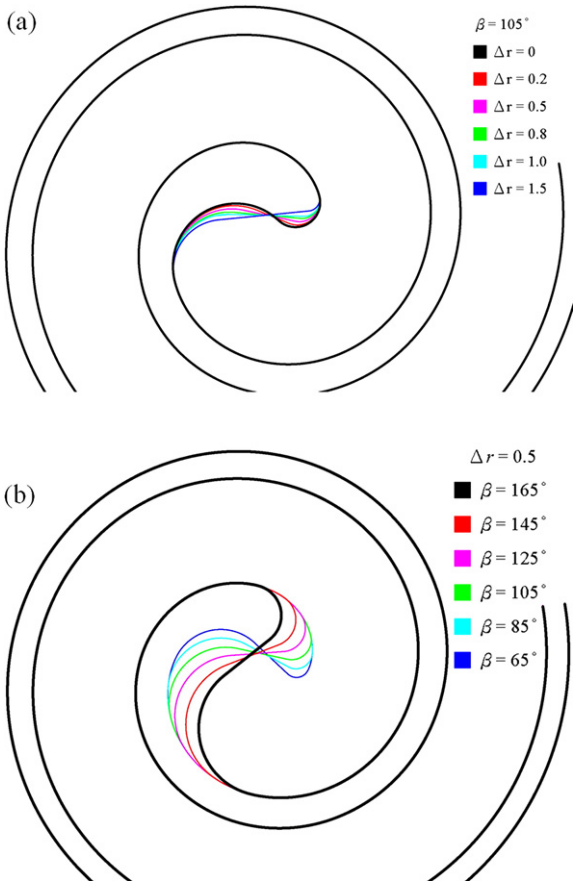

Fig. 11. (a) Comparison of different Δr values ($\beta = 105°(21\pi/36\text{rad})$). (b) Comparison of different β values ($\Delta r = 0.5\text{mm}$).

is shown in Fig. 11(b). Hence various parameter combinations and design varieties can be put in use to reform and improve the center portion of the scroll profile with these two modifications.

5. Conclusions

This study has developed one geometric model of scroll profiles which is constructed from an involute of circle with variable radii. Several case studies have been carried out to reveal important advantages that will result in higher efficiency, reliability and a more compact size of the STC. In addition, the arc and line modifications have also been studied in order to achieve perfectly meshing engagement at the center portion of the scroll profiles. Conclusions are summarized below:

1. A geometric model of the scroll profiles constructed from an involute of circle with variable radii has been built and the analytical expressions to the volume and its variation have been derived by designating the polytropic index $k=1$.
2. Smaller stress induced from the bending moment on the root of the scroll wrap and smaller deformation on the top of the scroll wrap will result if the scroll wrap height is lowered while keeping the suction volume, volume ratio and housing size the same as the conventional one. Therefore, the reliability and efficiency of STC can be improved.
3. One kind of these profiles with greater wrap thickness at the center and decreasing thickness from the inside outwards can provide better strength and rigidity. This profile suits STCs with operating pressures several times higher than the conventional ones.
4. More compact housing sizes of the STC can be achieved by this new type of profile when holding the suction volume, volume ratio and wrap height the same as the conventional profile. This provides wider design varieties in STC product development.
5. The arc and line modifications used in the conventional scroll profile can still be applied to this new scroll profile. Mathematic derivations and discussions regarding those modifications have been delivered in this study. The two most important purposes—avoiding interference at the center of the scroll pair and boosting the volume ratio to match the specified operating conditions—are both achieved by suitably choosing one of these two modifications, depending on design requirements.

Acknowledgements

The authors would like to express gratitude for financial support from the Energy and Environment Research Laboratories, Industrial Technology Research Institute in Taiwan. Appreciation is also expressed to the National Center for High-Performance Computing in Taiwan for its facility support.

References

[1] D.P. Gagne, J.J. Nieter, Simulating Scroll Compressors using a Generalized Conjugate Surface Approach, Proceedings of International Compressor Engineering Conference at Purdue, 1996, pp. 553–557.
[2] H. Mahfouz, M.N. Musa, M.N.B.W. Hassan, Theoretical Study on Scroll Compressor of New Hexagonal Involute, Proceedings of International Compressor Engineering Conference at Purdue, 2004, p. C073.
[3] T. Liu, Z.Q. Liu, Study on Geometry of Trigonometric-curve Modification of Scroll Profile for Scroll Compressor, Proceedings of International Compressor Engineering Conference at Purdue, 2004, p. C043.
[4] B. Wang, X. Li, W. Shi, A general geometrical model of scroll compressors based on discretional initial angles of involute, International Journal of Refrigeration 28 (2005) 958–966.
[5] Y.R. Lee, W.F. Wu, A study of planar orbiting mechanism and its applications to scroll fluid machinery, Mechanism and Machine Theory 31 (1996) 705–716.
[6] K. Terauchi, M. Hiraga, Scroll type fluid compressor with thickened spiral elements, US Patent 4547137 (1985).
[7] T. Hirano, K. Hagimoto, Scroll-type fluid machine with specific inner curve segments, US Patent 4856973 (1989).
[8] Y.R. Lee, W.F. Wu, On the profile design of a scroll compressor, International Journal of Refrigeration 18 (1995) 308–317.
[9] L.S. Li, P.C. Shu, Y.Z. Yu, The effect of scroll wraps on the performance of scroll compressors, International Journal of Refrigeration 20 (1997) 326–331.
[10] J. Gravesen, C. Henriksen, The geometry of the scroll compressor, Society for industrial and applied mathematics 43 (2001) 113–126.
[11] H. Bukac, The Theory of Scroll Profile, Proceedings of International Compressor Engineering Conference at Purdue, 2006, p. C080.
[12] J. Qiang, Study on basic parameters of scroll fluid machine based on general profile, Mechanism and machine theory 45 (2010) 212–223.
[13] K. Tojo, H. Ueda, Scroll type fluid compressor with an involute spiral based on a circle having a varying radius, US Patent 5425626 (1995).
[14] K. Tojo, H. Ueda, New wrap profile for scroll type machines, International Congress of refrigeration Proceedings 19 (1995) 515–521.
[15] T. Hirano, K. Hagimoto, Rotary type fluid machine, US Patent 4678415 (1987).
[16] Z. L. Fu, Y. Z. Yu, S. Y. Feng, Scroll compressor and other scroll machine, Xi'an Jiaotong University, book (1998) [in Chinese].
[17] S. Y. Feng, Modification and investigation in scroll curves of scroll compressor for vehicle conditioning, Xi'an Jiaotong University, master thesis (1998) [in Chinese].